International Conference on Space Optics—ICSO 2000

Toulouse Labège, France

5–7 December 2000

Edited by George Otrio

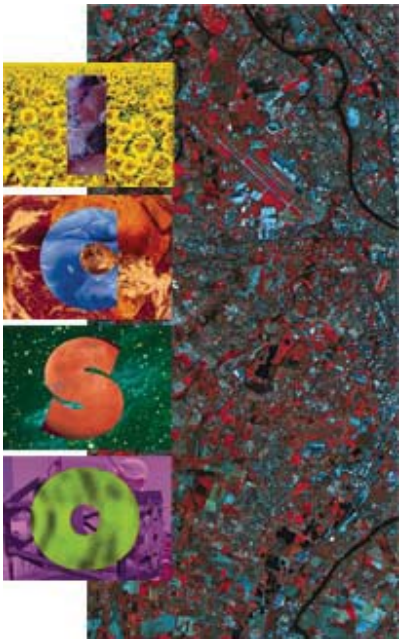

Multilayer four-flux model for the optical degradation of thermal control coatings in space

C. Tonon, C. Rozé, T. Girasole, Carole Duvignacq

International Conference on Space Optics — ICSO 2000, edited by George Otrio, Proc. of SPIE Vol. 10569
105691F · © 2000 ESA and CNES · CCC code: 0277-786X/17/$18 · doi: 10.1117/12.2307931

MULTILAYER FOUR-FLUX MODEL FOR THE OPTICAL DEGRADATION OF THERMAL CONTROL COATINGS IN SPACE

C. Tonon*, C. Rozé°, T. Girasole°, C. Duvignacq*

*ONERA/DESP, 2, avenue E. Belin, 31055 Toulouse Cedex , France
°UMR 6614-CNRS, Université et INSA de Rouen, LESP, BP08, 76131 Mont-Saint-Aignan Cedex, France

ABSTRACT *- The aim of this paper is to generalize the four-flux radiative transfer model to the case of a multilayer medium. An application is presented with the study of the optical degradation of a white paint in simulated space environment. This paint is constituted of a mixing a zinc oxide and a silicone resin. A sample was irradiated with 45 keV protons and reflectance measurements were achieved in situ after each step of irradiation in order to see the evolution of the thermo-optical properties of the coating. These tests were completed after irradiation by Scanning Electron Microscopy (SEM) in order to characterize the structure of the material and to detect possible structural changes due to the irradiation. This experimental investigation allowed us to define hypothesis to be introduced in the model. In particular, we assume that the optical degradation centered on 410 nm is due to a variation $\Delta\kappa$ of the imaginary part of the refractive index of zinc oxide in the damaged layer. The generalized four-flux model was validated by comparing numerical calculation with experiment.*

1. Introduction

During an orbital mission, measurement instruments, equipment and power supplies inside a spacecraft need to be in specific temperature conditions to correctly work. For this reason, a thermal control of the satellite must be provided. This can be passively done at the surface of the satellite by using coatings with special thermo-optical properties, defined by the solar absorptance α_s and the infrared emissivity ε. However, changes in these characteristics during exposure to the space environment have been a problem since they often conduct to an increase of the solar absorptance by the degradation of the optical properties of the coatings. Simulations in laboratory try to reproduce the degradation of materials in space environment but, as natural space is far too complex, simplifications must be done in the tests. Moreover, space projects involve very long mission duration, difficult to simulate on ground. For these reasons, physical comprehension of the phenomenon and predictive models are needed.

The model we present here reproduces optical changes observed in white space paints under particulate irradiation. We suppose that the yellowing of the white paint can be attributed to a change in the imaginary part of the refractive index of the material, which affects its absorption and scattering coefficients. In order to take into account this variation along the depth axis, we have to study this phenomenon using a multiple scattering model. Different scattering models may be used in order to solve the scattering transfer equation. One of them is the four-flux scattering model.

We present in this paper a generalization of this four-flux model to the case in which the medium is composed of an arbitrary number of layers. This model is then applied to the case of a white ZnO-paint. This paint is a thermal control coating, and its optical properties have to be known with accuracy.

2. Experiment

2.1 : Studied sample : white space paint

Samples that have been studied are white space paint samples. These coatings are composed of zinc oxide (ZnO) pigment particles, and a resin silicon binder (polydimethylsiloxane resin). The diameter distribution of the particles is evaluated from Scanning Electron Microscopy (SEM) observations, and is centered on 0,3 µm. The proportion in volume of the silicon resin in the paint is around 20 %. The total thickness of the paint is equal to 160 µm. The paint covers an aluminum substrate.

2.2 : Experimental apparatus:

Samples have been irradiated by 45 keV-protons (doses from 4.10^5 to 7.10^8 Gy), using the SEMIRAMIS facility (Ref 1). The facility is composed by a set of vacuum chambers pumped out with cryogenic pumping units allowing to reach a vacuum level of the order of 2.10^{-5} Pa. The system is connected to a solar UV simulator, two electron and proton Van de Graaf accelerators. Spectral reflectance of the material is measured for wavelengths between 250 and 2500 nm before and after irradiation. In order to avoid partial recovery effects due to air introduction in the chamber, these measurements were carried out in a secondary vacuum (better than 10^{-4} Pa) with a Perkin Elmer spectrophotometer, equipped with a lateral sample integrating sphere. The measurement error is equal to 1%.

2.3 : Study of the degradation and microscopy:

The evolution of the spectral reflectance is represented with the cumulated dose of 45 keV protons in (Figure 1).

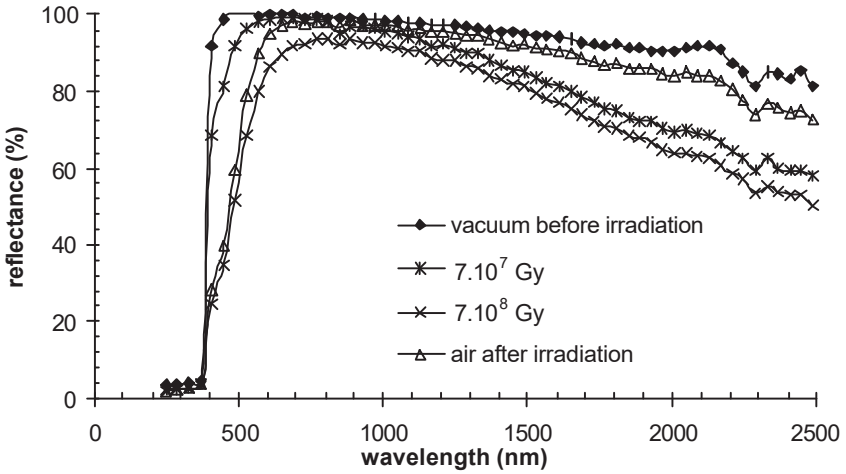

Figure 1 : Spectral reflectance a the white paint irradiated by 45 keV protons

Two regions are degraded under irradiation: the first one appears in the infrared region of the spectrum. This degradation nearly completely disappears when the sample is put back in air after irradiation. As this degradation is reversible, we could not determine its origin because of a lack of in situ characterization tests.

On another hand, spectral reflectance shows the appearance of a large absorption band at 410 nm for the proton-irradiated sample. This degradation is irreversible and is correlated with the yellowing of the material (Ref 2).

Once the sample was put back in air, we observed its structure by Scanning Electron Microscopy (SEM). SEM images obtained before and after irradiation of the paint with 45 keV-protons are shown in (Figure 2). The study of the sample before irradiation shows that it is

constituted of pigmented particles and vacuum. The particles are long-shaped and they are randomly oriented in the material. Their size distribution is centered on a diameter of 0.3 µm.

After irradiation, no change in the shape or size of the grains is observed. Therefore, the degradation seems to be not related to some topological parameters of powder particles.

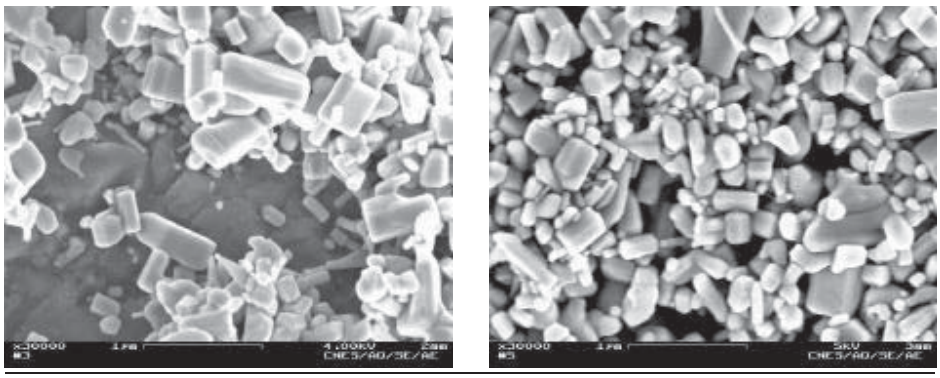

Figure 2 : SEM images of the paint before (left) and after (right) irradiation by 45 keV protons

3. Model

3.1 : Mie theory for a multilayered sphere

We see from SEM that the resin is invisible on images. In fact, it constitutes a very thin coating (about 5 % of the total radius of the particles for a volumic proportion of 20 %) embedding ZnO pigments and leading to their cohesion. Then, the embedding medium of this pigment/binder complex is vacuum. As a consequence, we model the particles of the paint by two-layer spheres embedded in vacuum. Their absorption coefficient k and scattering coefficient s are determined by a modified Lorenz-Mie theory (Ref. 3).

The geometry corresponding to the scattering of a plane wave or a Gaussian beam by a multilayered dielectric sphere is depicted in Figure 3. In this configuration, m_j is the complex refractive index of the material in the j^{th} layer relative to the refractive index of surrounding medium (Ref 3). The j^{th} layer is characterized by a size parameter of $x_j=2\pi r_j/\lambda$, where r_j is the outer radius of the layer j and λ is the wavelength of the incident wave in the surrounding free space.

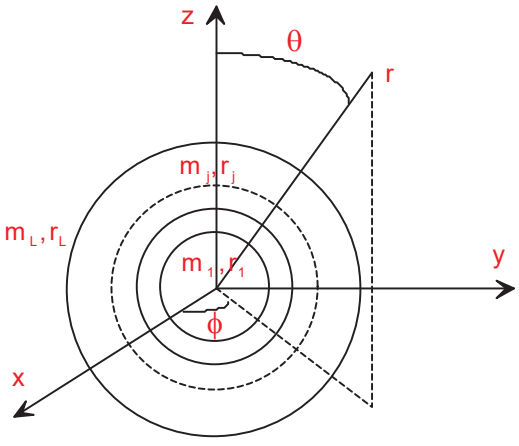

Figure 3 : Multilayered sphere geometry

The scattering coefficients a_n and b_n used in Lorenz-Mie theory can then be evaluated by use of a recursive computational scheme, taking the multilayered geometry into account (Ref 4). Once these coefficients are determined, we can deduce the different cross sections as a function of a_n and

b_n : C_{sca} is the scattering cross section, C_{abs} is the absorption cross section and C_{ext} is the extinction cross section, defined as the sum of C_{sca} and C_{abs}.

This leads to determine the absorption coefficient k and the scattering coefficient s:

$$\begin{aligned} k &= NC_{abs} = N(C_{ext} - C_{sca}) \\ s &= NC_{sca} \end{aligned} \tag{1}$$

where N is the particles density.

We applied the model, varying the size of the resin coating from 1 % to 30 % of the total radius of the particle. The comparison between calculation and experiment shows that a size of 5 % gives the best result with an error less than 2 %. This result confirms our hypothesis of such a multilayered system.

3.2 : Description of the four-flux model

During orbital missions, coatings used on spacecrafts are severely damaged by spatial environment. These missions being longer and longer, it becomes difficult to realize ground experiments in order to simulate optical degradation on coatings. In these conditions, predictive models are needed. They must allow us to predict optical property changes with irradiation dose. Moreover, they must be valid for the case of a dense material.

Multiple scattering theory, yet validated for coatings, allows calculating reflectance and transmittance values, and comparing them with experiment. It is interesting to obtain a simplification of this theory. Then, we have decided to use a four-flux model (Ref 6), derived from N-flux theories. This model is proved stricter than two-flux model of Kubelka-Munk (Ref 5), as it considers a specular component, contrary to Kubelka-Munk model. Moreover, this model permits to take nature of material into account, thanks to refractive indexes of matrix and pigmented particles. Particle size must be of the same order than incident light wavelength. Characteristics of the white paint studied here fit with four-flux model requirements. Therefore, this model has been chosen in order to study optical behavior of heterogeneous thermal control coatings (Ref 6, Ref 7).

We consider a slab (of infinite lateral extent) limited by planes (Z) and (O), which define a finite thickness, embedding discrete particles (Figure 4).

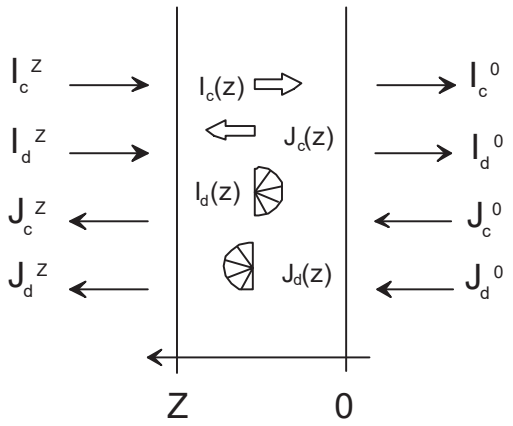

Figure 4 : Representation of the medium and the four flux

The incoming light on plane (Z) is constituted by a collimated beam I_c^Z and a semi-isotropic diffuse radiation I_d^Z. The incoming light on plane (0) is constituted by a collimated beam J_c^0 and a

semi-isotropic diffuse radiation J_d^0. Then, the whole radiation field at location z is modeled as a sum of four parts:

- a collimated beam of intensity $I_c(z)$ propagating to negative z,
- a collimated beam of intensity $J_c(z)$ propagating to positive z,
- a diffuse radiation $I_d(z)$ propagating to negative z,
- a diffuse radiation $J_d(z)$ propagating to positive z.

An approximation of the radiative transfer equation leads to:

$$\frac{dI_C}{dz} = (k+s)I_C \tag{2}$$

$$\frac{dJ_C}{dz} = -(k+s)J_C \tag{3}$$

$$\frac{dI_D}{dz} = -\zeta s I_C - (1-\zeta)\varepsilon s J_C + \varepsilon[k+(1-\zeta)s]I_D - \varepsilon(1-\zeta)s J_D \tag{4}$$

$$\frac{dJ_D}{dz} = (1-\zeta)\varepsilon s I_C + \zeta\varepsilon s J_C + \varepsilon(1-\zeta)\varepsilon s I_D - \varepsilon[k+(1-\zeta)s]J_D \tag{5}$$

where k is the absorption coefficient, and s the scattering coefficient. ζ represents the forward scattering ratio and is equal to the energy scattered by a volume element located at z in the forward hemisphere over the total energy for a given incident light angular distribution. ε is the average crossing parameter: when we consider an element of medium with a thickness dz, the average path length which is traveled over by the light is εdz.

Different terms in (2-5) are explained as follows:

- ζs is the forward scattering coefficient for a collimated radiation
- $\varepsilon\zeta s$ is the forward scattering coefficient for a diffuse radiation
- $(1-\zeta)s$ is the backward scattering coefficient for a collimated radiation
- $\varepsilon(1-\zeta)s$ is the backward scattering coefficient for a diffuse radiation
- εk is the absorption coefficient for a diffuse radiation

This equation system can be written under a matrix form:

$$\frac{d\bar{I}}{dz} = \bar{\bar{A}}\bar{I} = \begin{bmatrix} k+s & 0 & 0 & 0 \\ 0 & -(k+s) & 0 & 0 \\ -\zeta s & -(1-\zeta)\varepsilon s & \varepsilon[k+(1-\zeta)s] & -\varepsilon(1-\zeta)s \\ (1-\zeta)\varepsilon s & \zeta\varepsilon s & \varepsilon(1-\zeta)s & -\varepsilon[k+(1-\zeta)s] \end{bmatrix} \begin{bmatrix} I_c \\ J_c \\ I_d \\ J_d \end{bmatrix} \tag{6}$$

The solution is:

$$\bar{\bar{I}} = C_1\bar{x}_1 + C_2\bar{x}_2 + C_3\bar{x}_3 + C_4\bar{x}_4 \tag{7}$$

where $\bar{x}_1, \bar{x}_2, \bar{x}_3$ et $\bar{x}_4$ are the eigenvectors of matrix $\bar{\bar{A}}$, and C_1, C_2, C_3 and C_4 have to be determined by the boundary conditions.

Each limiting plane of the slab is a separation between different media, possibly having different optical index. Therefore, there are reflections at the interfaces between layers. Then, the flux Ic(Z) inside the layer at the plane (Z) is the sum of the transmitted external incident collimated flux IcZ through the interface and of the reflected outgoing flux Jc(Z). This can be written as:

$$I_c(Z) = (1 - r_c^Z)\, I_c^Z + r_c^Z J_c(Z) \tag{8}$$

Similar relations are expressed for diffuse and collimated fluxes at plane (0) and (Z):

$$\begin{aligned} I_d(Z) &= \left(1 - r_{de}^Z\right) I_d^Z + r_{di}^Z J_d(Z) \\ J_c(0) &= \left(1 - r_c^0\right) J_c^0 + r_c^0 I_c(0) \\ J_d(0) &= \left(1 - r_{de}^0\right) J_d^0 + r_{di}^0 I_d(0) \end{aligned} \tag{9}$$

where r_c^Z, r_{de}^Z, r_{di}^Z, r_c^0, r_{de}^0, r_{di}^0 are the different coefficients of reflection (Ref 7), I_d^Z is the incident diffuse flux on (Z), J_c^0 is the incident collimated flux on (0) and J_d^0 is the incident diffuse flux on (0) (see Figure 4).

These boundary conditions lead to determine constants C_1, C_2, C_3 and C_4. Knowing the incident collimated and diffuse flux, the outgoing fluxes I_c^0, I_d^0, J_c^Z and J_d^Z are written as:

$$\begin{aligned} I_c^0 &= \left(1 - r_c^0\right) I_c(0) + r_c^0 J_c^0 \\ J_c^Z &= \left(1 - r_c^Z\right) J_c(Z) + r_c^Z I_c^Z \\ I_d^0 &= \left(1 - r_{di}^0\right) I_d(0) + r_{de}^0 J_d^0 \\ J_d^Z &= \left(1 - r_{di}^Z\right) J_d(Z) + r_{de}^Z I_d^Z \end{aligned} \tag{10}$$

These equations can be rewritten in terms of reflectances and transmittances:

$$\begin{aligned} I_c^0 &= R_{cc}^0 J_c^0 + T_{cc} I_c^Z \\ J_c^Z &= T_{cc} J_c^0 + R_{cc}^Z I_c^Z \\ I_d^0 &= R_{cd}^0 J_c^0 + R_{dd}^0 J_d^0 + T_{cd}^Z I_c^Z + T_{dd}^Z I_d^Z \\ J_d^Z &= R_{cd}^Z I_c^Z + R_{dd}^Z I_d^Z + T_{cd}^0 J_c^0 + T_{dd}^0 J_d^0 \end{aligned} \tag{11}$$

where T_{cc} is the collimated-collimated transmittance, T_{cd} is the collimated-diffuse transmittance, T_{dd} is the diffuse-diffuse transmittance, R_{cc} is the collimated-collimated reflectance, R_{cd} is the collimated-diffuse reflectance and R_{dd} is the diffuse-diffuse reflectance. 0 and Z indicate each of the boundaries of the layer. Thanks to some algebra, these coefficients can be determined.

3.3 : Extension to the four-flux model for a multilayer plane medium:

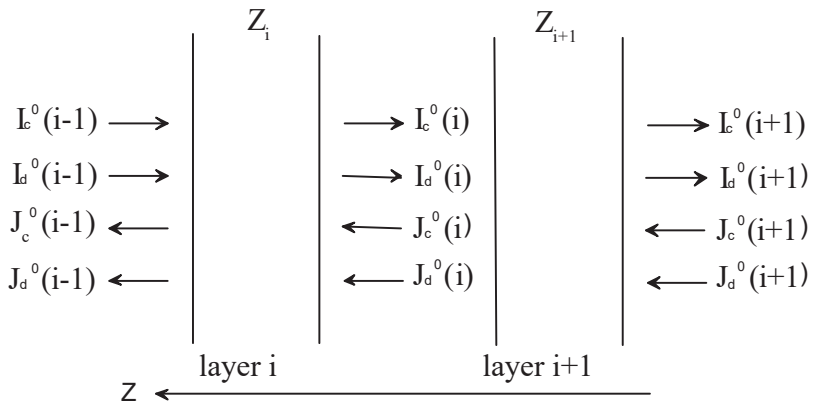

Figure 5 : Relations between a layer and neighboring layers

The case of multilayered material constitutes a generalization of the monolayered material case (Ref 7). We consider here that the material is composed of N layers of infinite lateral extent (Figure 5). In the layer i, outgoing flux is described versus the incident flux by:

$$\begin{aligned} I_c^z(i+1) &= T_{cc}(i)I_c^o(i-1) + R_{cc}^o(i)J_c^z(i+1) \\ I_d^z(i+1) &= T_{cd}^z(i)I_c^o(i-1) + T_{dd}^z(i)I_d^o(i-1) + R_{cd}^o(i)J_c^z(i+1) + R_{dd}^o(i)J_d^z(i+1) \\ J_d^o(i-1) &= R_{cd}^z(i)I_c^o(i-1) + R_{dd}^z(i)I_d^o(i-1) + T_{cd}^o(i)J_c^z(i+1) + T_{dd}^o(i)J_d^z(i+1) \\ J_c^o(i-1) &= R_{cc}^z(i)I_c^o(i-1) + T_{cc}(i)J_c^z(i+1) \end{aligned} \tag{12}$$

where i+1 represents the neighboring layer in negative z direction and i-1 represents the neighboring layer in positive z direction. I_c^z and I_d^z are respectively incident collimated and diffuse fluxes on plane (Z). J_c^o and J_d^o are respectively incident collimated and diffuse fluxes on plane (O). T_{cc} is the collimated-collimated transmittance, T_{cd} the collimated-diffuse transmittance, T_{dd} the diffuse-diffuse transmittance, R_{cc} the collimated-collimated reflectance, R_{cd} the collimated-diffuse reflectance, and R_{dd} the diffuse-diffuse reflectance. O and Z indicate each of the two boundaries of the layer.

Outgoing flux of a layer enter the neighboring layer, then:

$$\begin{aligned} I_c^z(i+1) &= I_c^o(i) \\ I_d^z(i+1) &= I_d^o(i) \\ J_c^z(i+1) &= J_c^o(i) \\ J_d^z(i+1) &= J_d^o(i) \end{aligned} \tag{13}$$

These relations lead to write system (13) under matrix form. Reflectance and transmittance coefficients are introduced in this matrix. Thanks to boundary conditions, fluxes at interfaces are determined from 4Nx4N-matrix inversion by Gauss transformation. In particular, the outgoing fluxes J_c^Z and J_d^Z are evaluated. Knowing the incident fluxes I_c^Z and I_d^Z, the total reflectance of the material is then given by:

$$R_{material} = \frac{J_c^Z + J_d^Z}{I_c^Z + I_d^Z} \tag{14}$$

4. Comparisons

4.1 : Initial white paint

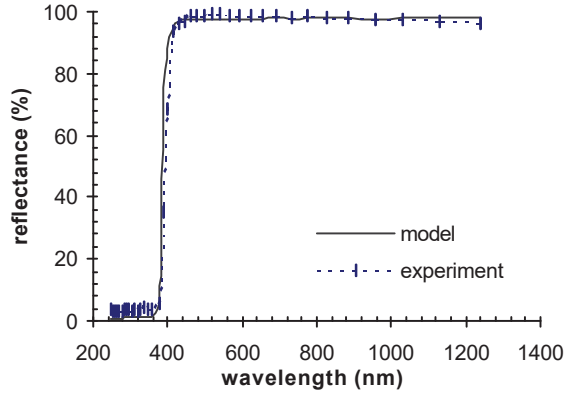

Figure 6 : Comparison between theoretical and experimental reflectance of the white paint

The four-flux model is applied considering a single layer medium. Figure 6 shows a comparison between theoretical and experimental reflectance of the white paint before irradiation. We observe a difference between the calculated reflectance and the measured one less than 2 %. This satisfactory result confirms the good behaviour of the model for this material.

4.2 : Irradiated white paint

Experimental investigation showed that the irradiation by charged particles causes the yellowing of the paint and the apparition of an absorption band centred on 410 nm. We assume that this degradation can be theoretically modelled by a variation $\Delta\kappa$ of the imaginary part of the refraction index of the zinc oxide pigment. This change appears in a thin layer near to the surface, which is defined by the penetration depth of the particles in the material and is equal to 0.8 µm. Consecutively, we have applied our model considering a two-layers system. The first layer is degraded, the second one is not affected by the irradiation and keeps its initial properties. The variation $\Delta\kappa$ is calculated in the degraded layer with a dichotomy method. The exit condition is fixed by a difference between the calculated reflectance and the experimental one less than 10^{-4}. Figure 7 shows the variation $\Delta\kappa$ of the imaginary part of the refractive index for several doses (4.10^5, 7.10^7 and 7.10^8 Gy).

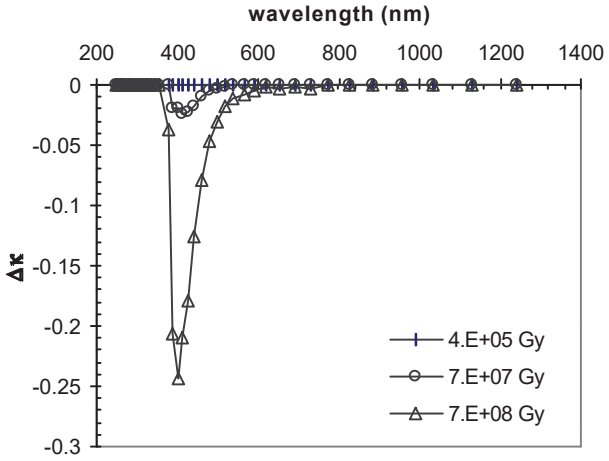

Figure 7 : Variation of the complex refractive index of zinc oxide in the degraded layer

We observe a strong change of $\Delta\kappa$ with the cumulated dose, with a maximum $\Delta\kappa_{max}$ at 410 nm, corresponding to the maximum of the absorption band in reflectance measurements. From these results, the maximum variation of the complex refractive index $\Delta\kappa_{max}$ was deduced as a function of the dose (Figure 8).

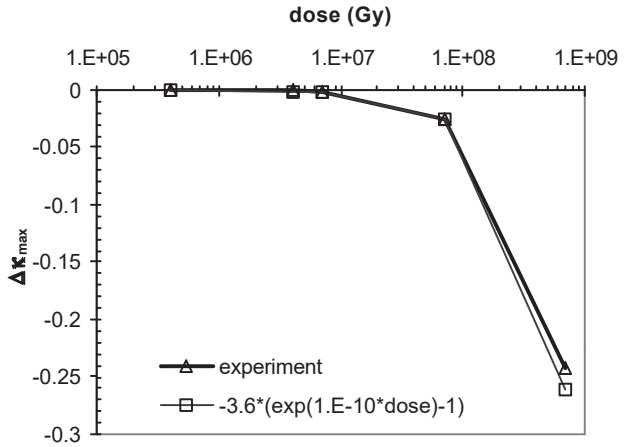

Figure 8 : Variation of the maximum of $\Delta\kappa$ with the dose

The difference between the degraded index and the initial one is very low for doses less than 10^7 Gy and then fastly increases with the dose. This can be modelled by an exponential law, chosen in order to take a possible saturation of the degradation into account. Indeed, the density of defects created during irradiation and responsible for the optical degradation is not infinite and probably reaches a maximum. This has already been observed during long-term laboratory simulations and we can expect the same kind of saturation for our saturation. We could reproduce this thanks to the exponential law:

$$\Delta\kappa_{max} = \Delta\kappa_0 \left(e^{\alpha d} - 1\right)$$

where $\Delta\kappa_0 = -3.6$, $\alpha = 10^{-10}$ and d is the dose. The coefficients $\Delta\kappa_0$ and α are determined to optimally fit the experimental curve. Unfortunately, we didn't observe the saturation during our experiment. This is why the law still has to be validated for doses greater than 10^9 Gy.

The law was then introduced in a predictive code, which evaluates the degradation for doses up to 10^9 Gy. We simulated the absorption band with a gaussian shape. The comparison between the calculation (Figure 9 a) and experiment (Figure 9 b) for three doses (4.10^5, 7.10^7 and 7.10^8 Gy) was made in the spectral range 250-1200 nm. This corresponds to the region where the refractive index of ZnO is well known. In this range, the error in the calculation is less than 10 %.

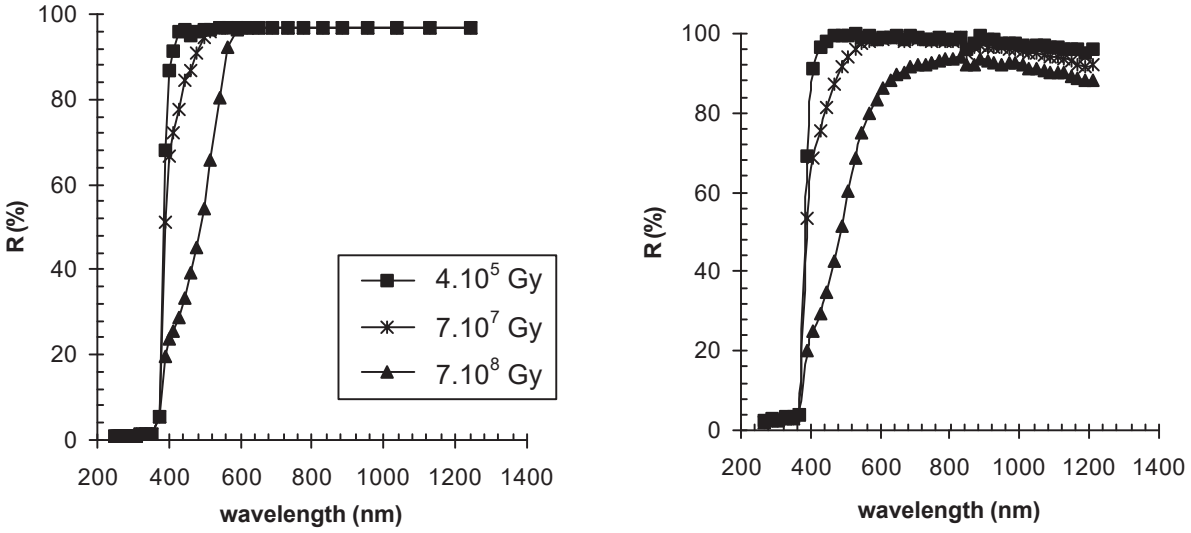

Figure 9 : (a) Calculated reflectance (predictive code) and (b) experimental reflectance

This result is very promising and should be improved in the future by introducing the infrared degradation in the numerical code.

5. Conclusion

Among all scattering models, it seems that four-flux scattering model is the most adapted for the study of paint's degradation. Indeed, this method which is derived from N-flux theory, permits to take physical characteristics of material (like particle size, material's refractive index and thickness…).

In this paper, we have proposed an extension of this classical four-flux model, for the case of a medium constituted of several layers, with different optical properties. This method has been applied to the case of a spatial white paint, irradiated by 45 keV-protons.

We have assumed that the observed yellow coloration and the apparition of a permanent absorption band in blue wavelengths can be explained by a variation of imaginary part of the refractive index in a thin surface layer of the paint. An empiric law for this variation is proposed, leading to saturation. Thanks to this law, a predictive model allows to calculate the reflectance for any dose by simulating the absorption band centered at 410 nm with a Gaussian shape.

More experiments have to be realized with higher doses in order to confirm the validity of the law describing the variation of refractive index. Moreover, the model have to be applied for different impacting particles, such as ultraviolet radiation or charged particles, with different energies.

References

Ref 1 : J. Marco, A. Paillous, F. Levadou, « Combined radiation effetc on optical reflectance of thermal control coatings », Proc. Of the 4th European Symposium on Spacecraft Materials in Space Environment, Toulouse, France, p. 121 (1988)

Ref 2 : J.M. Smith, W.E. Vehse, « ESR of electron irradiated ZnO confirmation of the F^+ center », Phys. Lett. A **31**, 147 (1970)

Ref 3 : Z.S. Wu, L.X. Guo, K.F. Ren, G. Gouesbet, G. Gréhan, « Improved algorithm for electromagnetic scattering of plane waves and shaped beams by multilayered spheres », Applied Optics, **36** (21), p.5188 (1997)

Ref 4 : F. Onofri, G. Gréhan, G. Gouesbet, « Electromagnetic scattering from a multilayered sphere located in an arbitrary beam », Applied Optics, **34** (30), p. 7113 (1995)

Ref 5 : P. Kubelka, F. Munk, « Ein Beitrag zur Optik der Farbanstriche », Z. Tech. Phys., **12**, p. 593 (1931)

Ref 6 : B. Maheu, J.N. Le Toulouzan, G. Gouesbet, « Four-flux models solve the scattering transfer equation in terms of Lorenz-Mie parameters », Applied Optics, **23** (19), p.3353 (1984)

Ref 7 : C. Tonon, C. Rozé, T. Girasole, M. Dinguirard, « Four-flux model for a multilayer plane absorbing and scattering medium : application to the optical degradation of a white paint in space environment », to be published in Applied Optics.